### Put paper number here

# MODEL PREDICTIVE CONTROL OF A LEAN-BURN GASOLINE ENGINE COUPLED WITH A PASSIVE SELECTIVE CATALYTIC REDUCTION SYSTEM

#### Qinghua Lin Pingen Chen

Tennessee Technological University Cookeville, Tennessee, 38505 Email: <a href="mailto:qlin42@students.tntech.edu">qlin42@students.tntech.edu</a>; pchen@tntech.edu

#### **ABSTRACT**

Lean-burn gasoline engines have demonstrated 10-20% engine efficiency gain over stoichiometric engines and are widely considered as a promising technology for meeting the 54.5 miles-per-gallon (mpg) Corporate Average Fuel Economy standard by 2025. Nevertheless, NO<sub>x</sub> emissions control for lean-burn gasoline for meeting the stringent EPA Tier 3 emission standards has been one of the main challenges towards the commercialization of highly-efficient lean-burn gasoline engines in the United States. Passive selective catalytic reduction (SCR) systems, which consist of a three-way catalyst and SCR, have demonstrated great potentials of effectively reducing NO<sub>x</sub> emissions for lean gasoline engines but may cause significant fuel penalty due to ammonia generation via rich engine combustion. The purpose of this study is to develop a model-predictive control (MPC) scheme for lean-burn gasoline engine coupled with a passive SCR system to minimize the fuel penalty associated with passive SCR operation while satisfying stringent NO<sub>x</sub> and NH<sub>3</sub> emissions requirements. Simulation results demonstrate that the MPCbased control can reduce the fuel penalty by 47.7% in a simulated US06 cycle and 32.0% in a simulated UDDS cycle, compared to the baseline control, while achieving over 96% deNOx efficiency and less than 15 ppm tailpipe ammonia slip. The proposed MPC control can potentially enable high engine efficiency gain for highly-efficient lean-burn gasoline engine while meeting the stringent EPA Tier 3 emission standards.

#### INTRODUCTION

In the U.S., the passenger car fleet is dominated by gasoline-powered vehicles. Gasoline accounted for 56% of total energy consumed by the U.S. transportation sector in 2015 and contributed over 40% of total CO<sub>2</sub> emissions from U.S. transportation activities in 2014 [1][2]. One of the most promising technologies for reducing fuel consumption from passenger cars is lean-burn gasoline engines, which have demonstrated over 10-20% fuel efficiency gain, compared to

#### Vitaly Y. Prikhodko

Fuels, Engines, and Emissions Research Center
Oak Ridge National Laboratory
Knoxville, Tennessee, 37932
Email: prikhodkovy@ornl.gov

stoichiometric engines, due to reduced heat losses and lower pumping loss [3]. However, nitrogen oxides (NO<sub>x</sub>) emissions control for lean-burn gasoline engines remains a great challenge, since traditional three-way catalysts (TWCs) which are standard NO<sub>x</sub> emission control devices for stoichiometric engines cannot effectively reduce NO<sub>x</sub> emissions in oxygenrich environment. Although lean NO<sub>x</sub> trap (LNT) and active urea-based selective catalytic reduction (SCR) system have been applied to Diesel engines, they have not been widely adopted for lean-burn gasoline engine applications due to high cost of catalyst for LNT and requirements of a sophisticated urea solution delivery system for urea-SCR systems [4].

To overcome these limitations, a cost-effective passive SCR system, which consists of a TWC (upstream) and a SCR (downstream), has been extensively investigated [4]-[6]. A passive SCR system utilizes reaction (1) on TWC for self-generating ammonia (NH<sub>3</sub>) during rich engine operation and stores the NH<sub>3</sub> in SCR downstream. The pre-stored NH<sub>3</sub> is utilized for NO<sub>x</sub> reduction during lean engine operation. To achieve effective NH<sub>3</sub> generation over TWC, a lean-burn gasoline engine needs to be operated in sufficiently rich combustion regime intermittently for producing sufficient hydrogen (H<sub>2</sub>) molecules in the engine exhaust. Furthermore, additional H<sub>2</sub> can be generated on TWC via water-gas-shift and steam-reforming mechanisms as described by reactions (2) and (3), respectively.

$$NO + 2.5H_2 \rightarrow NH_3 + H_2O$$
. (1)

$$CO + H_2O \leftrightarrow CO_2 + H_2$$
. (2)

$$C_3H_6 + 3H_2O \rightarrow 3CO + 6H_2$$
. (3)

1

It is reported that up to 99.7 % NO<sub>x</sub> conversion efficiency can be achieved by passive SCR systems at the specific engine operating conditions [7]. However, more research efforts are deserved for addressing the following critical technical barriers. First of all, the intermittent rich operation for NH<sub>3</sub> generation can deteriorate overall engine efficiency. Fuel penalty

associated with  $NH_3$  generation needs to be minimized to achieve maximum fuel efficiency gain from lean engine combustion. Secondly,  $NH_3$  generation on TWC and  $NH_3$  storage in downstream SCR system need to be closely coordinated. Excessive  $NH_3$  storage on the SCR can lead to unnecessary fuel penalty and high tailpipe  $NH_3$  slip, while insufficient  $NH_3$  storage can lower  $NO_x$  reduction efficiency. Thirdly, the stored  $NH_3$  needs to be fully utilized for enabling and sustaining highly-efficient lean-burn combustion modes and for reducing  $NO_x$  emissions during lean-burn operation. In addition, the durations of lean and rich operations as well as mode switching need to be optimized for achieving simultaneously high engine efficiency and low tailpipe  $NO_x$  emissions during transient driving cycles.

Since passive SCR systems have not been commercialized, the studies on these topics are still limited. Prikhodko et al., utilized a feedback control strategy based on cumulative NH<sub>3</sub> generated by the TWC during rich operation and NO<sub>x</sub> emissions during lean operation to evaluate the performance of a passive SCR system on lean gasoline research platform [7]. Plausible experimental results were achieved in the study, including greater than 99% NO<sub>x</sub> conversion efficiency and 6-11% fuel efficiency gain over stoichiometric operation at the steady-state engine operating conditions. However, with barely calibrations of lean/rich cycle timing based on the NH<sub>3</sub> storage and NH<sub>3</sub> consumption without fully incorporating engine operating conditions, the engine efficiency, combustion stability, and emissions are unlikely optimal in complex realworld driving cycles [4][7][8]. Instead, advanced model-based control systems that exploit the interaction of engine with aftertreatment systems are preferred.

The main contribution of this study is the development of model-predictive mode switching control that can simultaneously achieve high engine efficiency benefits and low tailpipe  $NO_x$  emissions and  $NH_3$  slip. Experiments were conducted to identify the optimal AFR ratio for  $NH_3$  generation, and to generate a map-based engine model and TWC model for enabling advanced model-predictive controls of lean-burn gasoline coupled with passive SCR system. The proposed model-predictive control was validated in simulation of US06 and UDDS cycles.

The rest of the paper is organized as follows. In the second section, the main operating principles of lean-burn gasoline engines and passive SCR system are briefly described. Then, test platform and experimental studies are discussed in the third section. Thereafter, engine and aftertreatment models are presented and MPC control is designed in the fourth section. In the fifth section, the simulation validation results of proposed MPC control are presented and discussed. Finally, concluding remarks are made at the end.

## MAIN OPERATING PRINCIPLES OF LEAN GASOLINE ENGINES AND PASSIVE SCR SYSTEMS

#### LEAN GASOLINE ENGINE OPERATING PRINCIPLE

Lean-burn gasoline engines mostly operate in one of the three modes including lean stratified mode, lean homogeneous mode, and stoichiometric homogeneous mode, depending on engine speeds and loads. Lean stratified mode provides the most engine efficiency gain (up to 20%) over stoichiometric operations and were generally employed in low-speed/low-load region with relative AFR, denoted as  $\lambda$  or lambda, ranging from 1.6-2.2. Lean homogeneous mode is generally applied in medium-speed/medium-load ranges with lambda in the range of 1.3-1.6. Stoichiometric homogeneous mode is generally applied at high speeds and high loads with lambda around 1.0. If a passive SCR system is applied to lean-burn gasoline engine for  $NO_x$  emission control, rich combustion mode is triggered intermittently for  $NH_3$  generation with lambda below 0.98.

#### TWC OPERATING PRINCIPLE

One of the critical functions for the TWC in a passive SCR system is NH<sub>3</sub> generation. The effectiveness of TWC as an NH<sub>3</sub> generator depends significantly on the exhaust gas compositions at TWC inlet and TWC temperatures. NO<sub>x</sub>-to-NH<sub>3</sub> conversion efficiency increases as the AFR decreases. Therefore, a rich engine combustion that results in high H<sub>2</sub>/NO<sub>x</sub> ratio in the exhaust, is preferred to achieve high NO<sub>x</sub>-to-NH<sub>3</sub> conversion efficiency. On the other side, as AFR ratio decreases, engine-out NO<sub>x</sub> emissions are reduced and thus NH<sub>3</sub> production is limited. In addition, engine efficiency decreases as AFR increases. Therefore, in NH<sub>3</sub> generation mode, AFR needs to be optimized for achieving high NH<sub>3</sub> production rate without incurring significant fuel penalty.

In addition, when engine is operated around stoichiometric AFR, engine-out  $NO_x$  emissions can also be reduced by TWC based on reaction (4).

$$CO + NO \rightarrow CO_2 + 0.5N_2$$
 (4)

#### PASSIVE SCR SYSTEM OPERATING PRINCIPLE

The main reactions governing a passive SCR catalyst are NH<sub>3</sub> adsorption and desorption on the catalyst surface as described by reaction (5), NO<sub>x</sub> reduction including "standard" SCR reaction as described in reaction (6) and "fast" SCR reaction as described in reaction (7), and NH<sub>3</sub> oxidation in (8) which takes place at high exhaust temperatures. While all these reactions may be simultaneously observed in urea-based SCR systems in Diesel applications, the governing reactions in the passive SCR depends significantly on the exhaust condition since lean gasoline engines may operate in lean, stoichiometric, or rich exhaust condition. When engine is operated in lean combustion modes (lean stratified mode or lean homogeneous mode), no NH<sub>3</sub> is generated on TWC and thus the NH<sub>3</sub> adsorption does not exist in such case. When engine is operated in rich combustion mode for NH<sub>3</sub> generation, NO<sub>x</sub> can primarily be converted into NH3 on TWC and no O2 molecules are available in the exhaust, and thus reactions (6) and (7) can be ignored. When engine is operated in stoichiometric mode,

most of engine-out  $NO_x$  emissions are converted into nitrogen on TWC. As a result, neither  $NO_x$  reduction nor  $NH_3$  adsorption can be observed in SCR system.

$$NH_3 + \theta_{free} \leftrightarrow NH_3^*$$
 (5)

$$4NH_3^* + 4NO + O_2 \rightarrow 4N_2 + 6H_2O$$
. (6)

$$2NH_3^* + NO + NO_2 \rightarrow 2N_2 + 3H_2O$$
. (7)

$$2NH_3^* + 1.5O_2 \rightarrow N_2 + 3H_2O$$
. (8)

#### **TEST PLATFORM AND EXPERIMENTAL STUDY**

#### TEST PLATFORM AND INSTRUMENATIONS

The test platform used in this study is a 4-cylinder 2.0L naturally aspirated direct injection lean-burn gasoline engine from a MY 2008 BMW 120i vehicle at Oak Ridge National Laboratory. The original engine control unit (ECU) was replaced by a new ECU which provides full control of the engine parameters such as air/fuel ratio (AFR), fuel injection timing and rate, sparking timing, EGR ratio, and others. The aftertreatment system is composed of a 1.3L closed-coupled TWC without oxygen storage capacity and a 2.5 L Cu-zeolite SCR placed in an under-floor position downstream of the TWC. The schematic of the integrated lean-burn gasoline engine and passive SCR system is shown in Figure 1.

The main emission measurement systems include a MKS Instruments MultiGas Model 2030 HS FTIR spectrometers for simultaneous measurements of various gas species such as CO, NO, NO<sub>2</sub>, N<sub>2</sub>O, NH<sub>3</sub>, at two different sampling points, a California Analytical Instruments (CAI) heated flame ionization detector (FID) for total unburned hydrocarbons measurement. Details about the test platform and emission sampling can be found in [7]. In addition to exhaust gas analyzers, pressure sensors, thermocouples, and universal exhaust gas oxygen (UEGO) sensors are available at various locations.

#### Lean-burn gasoline engine

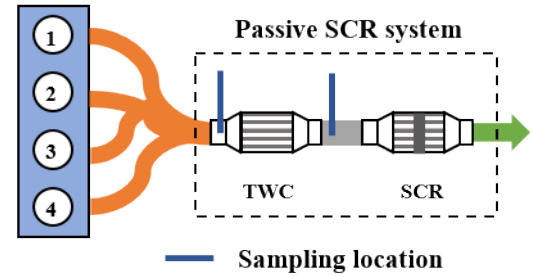


Figure 1 Schematic of Engine-Passive SCR Platform.

#### EXPERIMENT STUDY AND DISCUSSIONS

Since intermittent rich combustion mode is needed for  $NH_3$  generation for the passive SCR system and the rich combustion can incur additional fuel penalty, it is critical to optimize  $\lambda$  from both fuel penalty and  $NH_3$  generation standpoints. A lower  $\lambda$  than needed can lead to higher fuel penalty and lower engine-out  $NO_x$  emissions and thus limited  $NH_3$  production, while a higher  $\lambda$  than needed can improve engine efficiency

but reduce  $H_2$  content and thus lower  $NH_3$  generation rate on TWC. In addition, if  $\lambda$  is further increased close to the stoichiometric value ( $\lambda$ =1.0),  $NO_x$ -to- $NH_3$  conversion efficiency drops significantly since most of engine-out  $NO_x$  emissions are selectively converted into nitrogen on TWC.

To investigate the impact of AFR (i.e.,  $\lambda$ ) on the fuel penalty associated with NH<sub>3</sub> generation and NO<sub>x</sub>-to-NH<sub>3</sub> conversion efficiency on TWC, three steady-state AFR sweep tests were conducted at 2000 rpm with three brake mean effective pressure (BMEP) at 3 bar, 5 bar, and 8 bar, respectively. As shown in Table 1,  $\lambda$  was ranged from 0.92 to 1.05 in each test, while the other engine parameters are maintained the same. External EGR was disabled for maximizing the engine-out NO<sub>x</sub> emissions. The two FTIR sampling benches were placed at engine outlet and TWC outlet, respectively, for measuring the exhaust emissions. The engine was operated at each  $\lambda$  until the emissions at the engine outlet and TWC outlet were stable.

According to the prior experimental study in [9] with the original ECU, to achieve the maximum engine efficiency the engine is operated in lean-stratified mode with  $\lambda = 1.76$  at 2000 rpm/3 bar, and in lean homogeneous mode with  $\lambda = 1.46$  at 2000 rpm/5 bar. The corresponding fuel consumption rates and exhaust emissions at 2000 rpm/3 bar and 2000 rpm/5 bar were adopted in this study as the references for computing the fuel penalty associated with NH<sub>3</sub> generation. At 2000 rpm/8 bar,  $\lambda = 1.0$  was taken as the reference value for calculating the fuel penalty

**Table 1 Test Procedure during AFR Sweep Tests** 

Speed (rpm)	BMEP(bar)	Relative AFR ( $\lambda$ )
2000	3	$0.92-1.0 (\Delta=0.1), 1.05, 1.76*$
	5	$0.92-1.0 (\Delta=0.1), 1.05, 1.46*$
	8	0.92-1.05, 1.0*

<sup>\*</sup> denotes the reference relative AFR,  $\lambda_r$ .

Figure 2 shows the fuel penalty with respect to the reference  $\lambda$  at different BMEPs. As seen in Figure 2, fuel penalty decreases as  $\lambda$  increases in the range from 0.92 to 1.05 for all three BMEPs. Compared to the fuel penalty at 3 bar, the fuel penalty at 8 bar is 12% to 60% lower when  $\lambda$  varies from 0.92 to 0.97. This is due to the fact that, at a low BMEP, engine efficiency is significantly higher in lean stratified mode than in NH<sub>3</sub> generation mode, while the engine efficiency gap between the stoichiometric mode and NH<sub>3</sub> generation mode is smaller at a high BMEP than at a low BMEP. This figure indicates that engine operations with a high BMEP is preferred over engine operations with a low BMEP for NH<sub>3</sub> generation due to the lower fuel penalty.

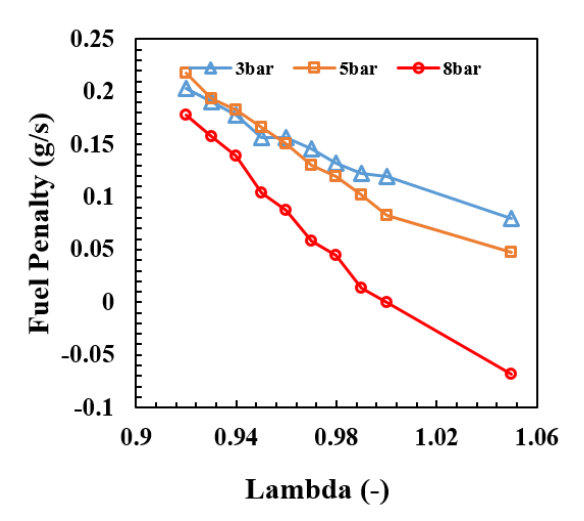


Figure 2 Fuel Penalty vs  $\lambda$  at 2000 rpm (3bar, 5bar, 8bar).

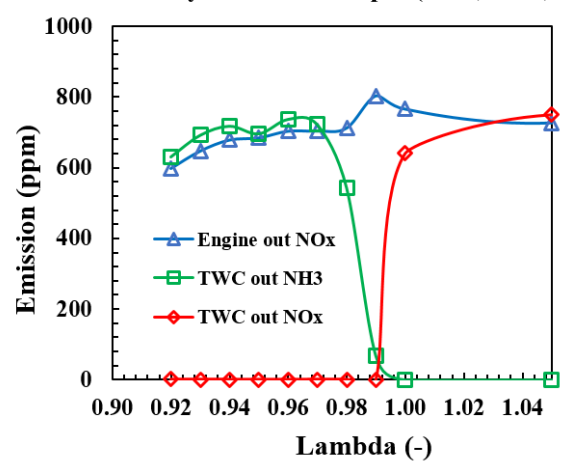


Figure 3 Impact of  $\lambda$  on NO<sub>x</sub>-to-NH<sub>3</sub> Conversion on TWC at 2000 rpm/3 bar.

Figure 3 and Figure 4 show the impact of  $\lambda$  on the NO<sub>x</sub>to-NH<sub>3</sub> conversion on TWC with  $\lambda$  ranging from 0.92 to 1.05 at 2000 rpm/3 bar and 2000 rpm/8 bar, respectively. As can be seen from Figure 3, complete NO<sub>x</sub>-to-NH<sub>3</sub> conversion can be achieved when  $\lambda \le 0.97$ . The peak TWC-out NH<sub>3</sub> emissions were observed around  $\lambda = 0.96$  and dropped slightly when  $\lambda = 0.97$ . As  $\lambda$  increases from 0.98 to 0.99, the NO<sub>x</sub>-to-NH<sub>3</sub> conversion becomes very limited, while TWC-out NO<sub>x</sub> emissions remain zero, which indicates effective NO<sub>x</sub>-tonitrogen conversion on TWC. As  $\lambda$  further increases to 1.05, the TWC becomes ineffective in reducing NO<sub>x</sub> emissions. Similarly, as can be seen from Figure 4, TWC-out NH<sub>3</sub> concentration reaches the peak value around  $\lambda = 0.96$  and then drop slightly around  $\lambda = 0.97$ . On the other hand, less fuel penalty can be achieved at  $\lambda = 0.97$  than at  $\lambda = 0.96$  for both 3 bar and 8 bar. Therefore, considering the trade-off between NH<sub>3</sub> production and the associated fuel penalty, the most costeffective  $\lambda$  for NH<sub>3</sub> generation was selected as 0.97 in this study. On the other side, the optimal  $\lambda$  in NH<sub>3</sub> consumption

mode is 1.76, 1.46, and 1.0 for 2000 rpm/3 bar, 2000 rpm/5 bar, 2000 rpm/8 bar, respectively, as shown in Table 1.

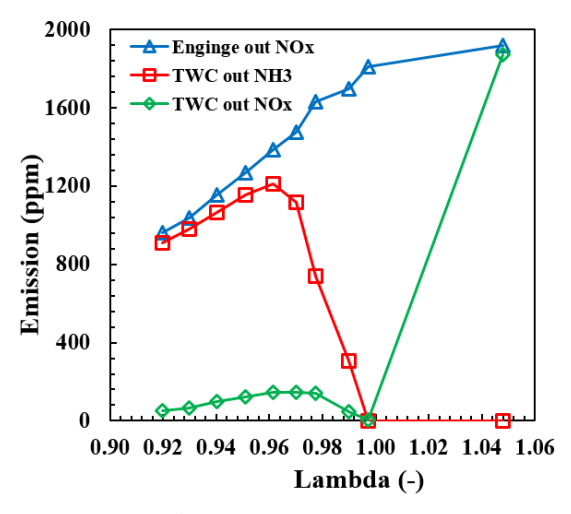


Figure 4 Impact of  $\lambda$  on NO<sub>x</sub>-to-NH<sub>3</sub> Conversion on TWC at 2000 rpm/8 bar.

#### MODEL PREDICTIVE MODE SWITCHING CONTROL

The optimization of AFR for the lean-burn gasoline engine coupled with passive SCR system consists of two main tasks. The first task is the optimization of AFR in NH<sub>3</sub> generation mode and AFR in NH<sub>3</sub> consumption mode at specific engine operating points, which can be achieved from the experimental studies as demonstrated in the prior section. The second task is the optimization of lean/rich cycling timings for maximizing lean-burn gasoline engine efficiency benefits. This section mainly focuses on developing a systematic framework for achieving the second task. The lean/rich mode switching depends significantly on the NH<sub>3</sub> storage level on the SCR catalyst, which can be quantified by NH<sub>3</sub> surface coverage ratio as defined in (5).

$$\theta = \frac{M_{NH_3}}{\Theta},\tag{5}$$

where  $M_{NH_3}$  denotes the amount of NH<sub>3</sub> adsorbed on the catalyst sites;  $\Theta$  is the NH<sub>3</sub> storage capacity.

If sufficient NH<sub>3</sub> is stored on the SCR catalyst for future NO<sub>x</sub> reduction, lean-burn gasoline engine can operate in highly efficient lean modes. Otherwise, the lean gasoline engine is forced to operate in NH<sub>3</sub> generation mode which may incur high fuel penalty. As mentioned in the previous section, high BMEP is preferred for NH<sub>3</sub> generation due to lower fuel penalty, while low BMEP is preferred for lean operation which provide the most fuel efficiency gain over stoichiometric operation. Therefore, the control objective is to achieve relatively high NH<sub>3</sub> storage level at the end of high-speed/high-torque operation, and relatively low NH<sub>3</sub> storage level towards the end of low-speed/low-torque operation. It is of great challenge to achieve aforementioned control objective due to the high complexity of real-world driving cycle. Model-predictive control, which is capable of utilizing the previewed

input information and model-based prediction of system behaviors for optimizing the defined cost function, is an ideal tool for realizing the control objective. First of all, the control-oriented engine and aftertreatment models are briefly described in the first subsection. Then, the development of MPC-based model switching control is discussed.

#### ENGINE AND PASSIVE SCR MODELS

In this simulation study, the engine model incorporates different maps which were obtained from AFR sweep experiments mentioned in the prior section, including engineout NO<sub>x</sub> concentration map, engine-out O<sub>2</sub> concentration map, engine-out exhaust flow rate map, engine fuel penalty map, and others. A map-based TWC model was applied in this simulation study as well. The embedded maps are also obtained from the AFR sweep tests. The key maps include NO<sub>x</sub>-to-NH<sub>3</sub> conversion efficiency map, engine-out O<sub>2</sub> concentration map, TWC-out exhaust flow rate map, and TWC-out exhaust temperature map. A control-oriented four-state SCR model was originally developed and experimentally validated by The Ohio State University in [10]. The original SCR model was simplified into the following three-state SCR model by ignoring the fast SCR reaction in (9) based on the experimental observation that the TWC-out NO<sub>2</sub>/NO<sub>x</sub> is generally less than

$$\begin{bmatrix} \mathbf{c}_{NO}^{\mathbf{c}} \\ \mathbf{c}_{NO}^{\mathbf{c}} \end{bmatrix} = \begin{bmatrix} -C_{NO}(r_{red}\Theta\theta C_{O_2}V + \frac{F}{V}) + \frac{F}{V}C_{NO,in} \\ -C_{NH_3} \left[\Theta r_{ads}(1-\theta) + \frac{F}{V}\right] + \frac{r_{des}\Theta\theta}{V} + \frac{F}{V}C_{NH_3,in} \\ (1-\theta)r_{ads}C_{NH_3}V - \theta(r_{des} + r_{red}C_{NO}C_{O_2}V^2) \end{bmatrix}, \quad (9)$$

where  $C_{NO}$ ,  $C_{NH_3}$ , and  $C_{O_2}$  are the NO concentration, NH<sub>3</sub> concentration, and O<sub>2</sub> concentration inside the SCR system, respectively;  $r_x = k_x \exp\left[-E_x/\left(RT_{SCR}\right)\right]$  where x={red, ads, des}, and the values of  $k_x$  and  $E_x$  are constants;  $T_{SCR}$  denotes the exhaust gas temperature at the SCR outlet; V represents the volume of SCR system;  $C_{NO,in}$  and  $C_{NH_3,in}$  represent the NO and NH<sub>3</sub> concentrations at the SCR inlet, respectively; F is the exhaust gas flow rate;  $\Theta$  is modeled as a function of exhaust gas temperature.

#### MPC CONTROLLER DESIGN

The overall schematic of MPC controller is shown in Figure 5. The cost function to be minimized by the MPC consists of three parts. The first part represents the fuel cost caused by NH<sub>3</sub> generation during the prediction horizon. The second part represents the equivalent fuel cost due to the NH<sub>3</sub> consumption in the SCR system. This part is added to the cost function due to the fact that, for the passive SCR system, NH<sub>3</sub> is generated at a certain fuel penalty. The third part represents the terminal cost which is applied only when there is a change of BMEP within the complete prediction horizon. The terminal cost is designed to encourage NH<sub>3</sub> consumption at a lower

BMEP due to higher engine efficiency gain and higher fuel penalty for NH<sub>3</sub> generation before BMEP is shifted to a higher value. Similarly, the terminal cost is also designed to encourage NH<sub>3</sub> generation at a higher BMEP due to lower fuel penalty. In addition to the cost function, it is required that  $\theta$  during lean operation to be above the minimum bound ( $\theta_{\rm min}$ ) for achieving the desired NO<sub>x</sub> reduction efficiency and  $\theta$  to be below the maximum bound ( $\theta_{\rm max}$ ) to avoid excessive NH<sub>3</sub> slip [11]. The cost function in the receding horizon is formulated in (10).

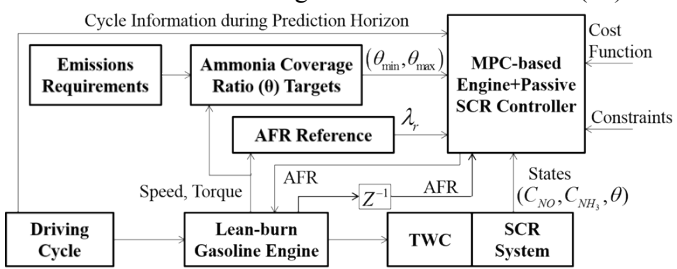


Figure 5 MPC-based AFR Control Scheme.

$$J = \min\{\sum_{i=1}^{n} (\mathbf{n}_{f_{iuel}}^{\mathbf{n}}(i) - \mathbf{n}_{f_{i}}^{\mathbf{n}}(i)) + k_{1}(\Theta(1)\theta(1) - \Theta(n)\theta(n)) + J_{t}\}$$
(10)

where  $n = \min\left\{N, N_{up}, N_{dn}\right\}$ ; N is the length of a complete prediction horizon;  $N_{up}$  and  $N_{dn}$  denotes the time instants when the BMEP is changed to a higher value and a lower value, respectively;  $n_{fuel}(i)$  and  $n_{fuel}(i)$  are the fuel mass flow rate (g/s) with  $\lambda(i)$  and reference fuel mass flow rate (g/s), respectively;  $k_1$  and  $k_2$  are constant weighting factors to be designed; J, represents the terminal cost.

$$J_{c} = \begin{cases} 0, & \text{if } n=N \\ k_{2} |\theta(n) - \theta_{t}(n)|, & \text{if } n < N \end{cases},$$

$$\theta_{t}(n) = \begin{cases} \theta_{\min}(n), & \text{if } BMEP(i) < BMEP(i+1) \\ \theta_{\max}(n), & \text{if } BMEP(i) > BMEP(i+1) \end{cases}.$$
Constraints:

$$\begin{split} & \lambda_{\min}\left(i\right) < \lambda(i) < \lambda_{\max}\left(i\right) \\ & \theta_{\min}\left(i\right) \leq \theta(i) \leq \theta_{\max}\left(i\right), \quad if \ \lambda(i) > 1.0 \ . \\ & \theta(i) \leq \theta_{\max}\left(i\right), \qquad if \ \lambda(i) \leq 1.0 \end{split}$$

The design variable is the mode switching time, denoted as  $N_{sw}$ . To avoid excessive mode switching, it is assumed that at most one lean-to-rich switching and one rich-to-lean switching is allowed in the optimization horizon. The corresponding  $\lambda(i)$  is designed as below.

$$\lambda(i) = \begin{cases} \lambda^{C}(0), & \text{if } i > N_{sw} \\ \lambda(0), & \text{else} \end{cases},$$

where  $\lambda(0)$  denotes  $\lambda$  applied in the previous step or a predefined  $\lambda$  if it is the start of a new engine operation;

 $\lambda^{C}(0)$  represents the complement of  $\lambda(0)$  in the set  $U(i) = \{0.97, \lambda_r(i)\}$ .

After the design of cost function, the next step is the systematic design of weighting factors  $k_1$  and  $k_2$ . Figure 6 and Figure 7 demonstrate the impact of  $k_1$  on the cost function at 2000 rpm/3 bar and 2000 rpm/8 bar, respectively, without considering the terminal cost and constraints. For 2000 rpm/3 bar,  $k_1$  is designed such that minimum cost function is found at  $\lambda = 1.79$ , which means engine is operated in lean stratified mode by minimizing the cost function until  $\theta_{\min}$  is reached. On the other hand,  $k_1$  is designed such that the local minimum of the cost function is located around 0.97 which is known as the optimal  $\lambda$  for NH<sub>3</sub> generation. According to the cost function profiles shown in Figure 6, only  $k_1 = 100$  meets the design criteria. For 2000 rpm/8 bar, NH3 generation mode is encouraged, which indicates that  $k_1$  should be designed such that the global minimum is located at  $\lambda = 0.97$ . According to cost function profiles, one can see that  $k_1 = 100$  again meet the design criterion. Therefore, based on the detailed cost function analysis,  $k_1$  is selected to be 100. A large  $k_2$  is designed to minimize the terminal cost which is  $|\theta - \theta_{\min}|$  at the end of lowspeed/low-load operation, or  $|\theta - \theta_{\text{max}}|$  at the end of highspeed/high-load operation.

In addition, different  $\theta_{\rm max}$  values are designed for different engine operating regimes. A lower  $\theta_{\rm max}$  is assigned at low-speed/low-load operation (e.g., 2000 rpm/3 bar) to encourage NH<sub>3</sub> consumption due to higher engine efficiency benefit, while a higher  $\theta_{\rm max}$  is assigned at high-speed/high-load operation (e.g., 2000 rpm/8 bar) for encouraging NH<sub>3</sub> generation due to lower fuel penalty.

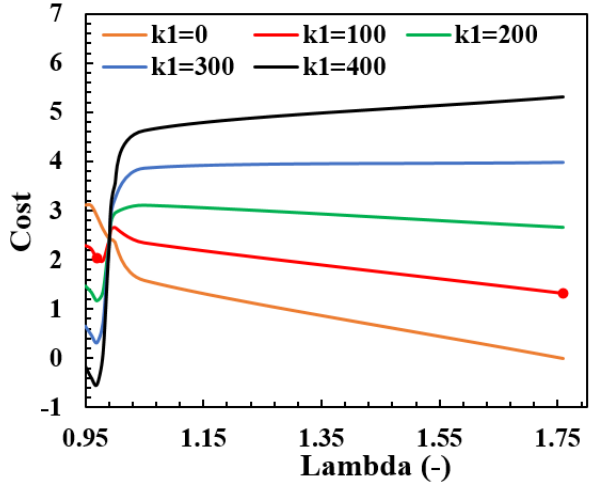


Figure 6 Effect of  $k_1$  on Cost Function at 2000 rpm/3 bar.

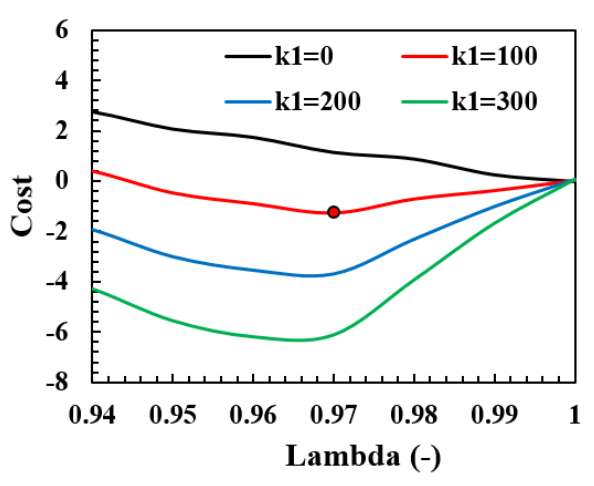


Figure 7 Effect of  $k_1$  on Cost Function at 2000 rpm/8 bar.

#### SIMULATION RESULTS AND ANALYSIS

In this section, the proposed MPC-based mode switching control was verified in simulation in two transient driving cycles with torque switching patterns similar to US06 and UDDS cycles. Since AFR sweep tests were performed only at 2000 rpm as shown in the experimental study section, the engine exhaust information and fuel penalty associated with NH<sub>3</sub> generation for other engine speeds and BMEPs are not available at this moment. Instead, the engine operation in US06 cycle was classified into two categories: high-torque operation and low-torque operation. The pattern of switching between high-torque operation and low-torque operation was extracted from US06 cycle. The switching pattern was also extracted from UDDS cycle using a similar approach. Then, two new cycles with constant speed at 2000 rpm and two BMEPs (3bar and 8bar) were designed based on the switching patterns extracted from US06 cycle and UDDS cycle, as shown in Figure 8. The two cycles were named "US06" and "UDDS", respectively. For the MPC controller,  $\theta_{\max}$  was designed to be 0.15 and 0.25 for 2000 rpm/3 bar and 2000 rpm/8 bar, respectively, while  $\theta_{\min} = 0.10$  is applied for both BMEPs. The  $\theta_{\min}$  and  $\theta_{\max}$  were designed based on model-based reference design approach in [11] to achieve over 95% deNOx efficiency and less than 15 ppm tailpipe NH3 slips. The length of prediction horizon was selected as 20 seconds.

For comparison purpose, a  $\theta$ -based mode-switching controller was created as the baseline control. For the baseline control, the engine is operated in one mode and the mode switching takes place only when  $\theta$  reaches the upper bound ( $\theta_{\text{max}} = 0.25$ ) or the lower bound ( $\theta_{\text{min}} = 0.10$ ). In NH<sub>3</sub> generation mode,  $\lambda = 0.97$  was applied, while in NH<sub>3</sub> consumption mode, the reference  $\lambda_r$  in Table 1 was applied.

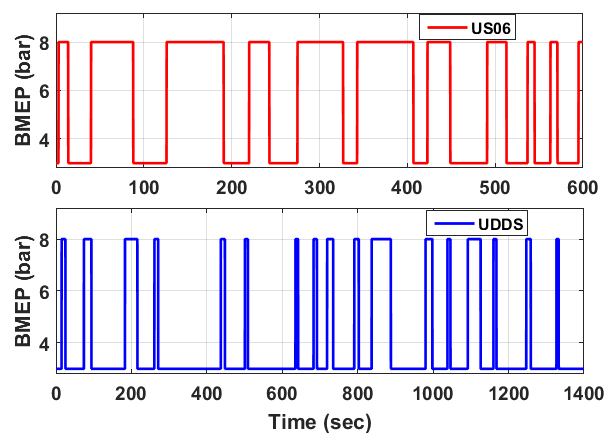


Figure 8 Simulated US06 Cycle (top) and Simulated UDDS Cycle (bottom).

Figure 9 and Figure 10 compare  $\theta$  and  $\lambda$  trajectories, respectively, over the simulated US06 cycle. It can be seen from Figure 10 that a wave-like trajectory was resulted with the baseline control, while the MPC-based control is more selective in terms of NH<sub>3</sub> production and consumption timings. The MPC control is capable of fully utilizing 2000 rpm/8 bar as the cost-effective  $NH_3$ generation region. In addition, implementation of a terminal cost in MPC encourages high NH<sub>3</sub> storage level at the end of high-torque operation. The prestored NH3 allows engine to operate in lean stratified mode at 2000 rpm/3 bar during the simulated US06 cycle, as demonstrated clearly in Figure 10. As a result, maximum engine efficiency gain was achieved. In comparison, since the baseline control is governed by simple mode switching logic which did not allow mode switching until the upper bound or lower bound is reached, it forced engine to operate in rich mode even at 2000 rpm/3 bar, which resulted in higher fuel penalty. It can be seen from Figure 9 that the  $\theta$  from both MPC control and baseline control are within the upper bound and lower bound, which indicates the tailpipe NH<sub>3</sub> slip and NO<sub>x</sub> conversion efficiency requirements are satisfied.

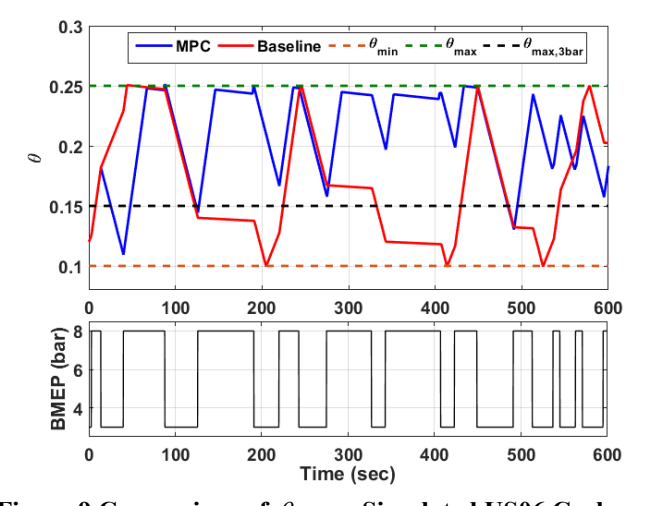


Figure 9 Comparison of  $\theta$  over Simulated US06 Cycle.

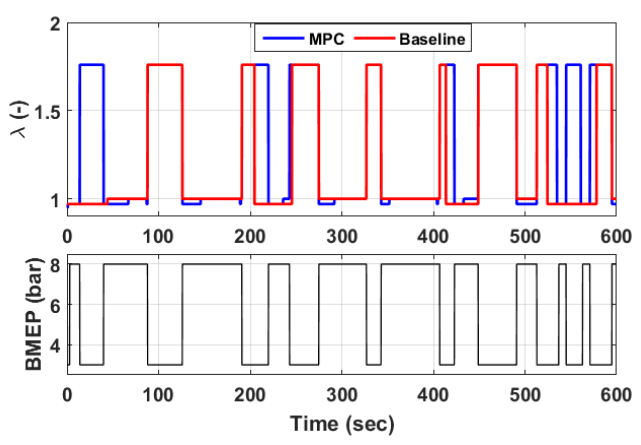


Figure 10 Comparison of  $\lambda$  over Simulated US06 Cycle.

Table 2 compares the corrected fuel penalty (including fuel penalty and equivalent fuel penalty due to NH<sub>3</sub> consumption), NO<sub>x</sub> conversion efficiency, and average NH<sub>3</sub> slip for simulated US06 and UDDS cycles. Both MPC control and baseline control can achieve over 96% NO<sub>x</sub> conversion efficiency and less than 15 ppm NH<sub>3</sub> slip on average during US06 cycle. However, MPC is capable of achieving 47.7% less fuel penalty than the baseline control.

Table 2 Comparison of Baseline Control and MPC Control.

Cycle	Controller	Fuel	$NO_x$	Average
		penalty	conversion	NH <sub>3</sub> slip
		(g)	efficiency (%)	(ppm)
US06	Baseline	16.28	98.0	10.7
	MPC	8.51	96.6	13.8
UDD	Baseline	107.13	97.9	11.2
S	MPC	72.81	96.1	8.6

Figure 11 and Figure 12 demonstrate  $\theta$  and  $\lambda$  trajectories, respectively, over the simulated UDDS cycle. One can see from Figure 11 that the baseline control resulted in a bigger wavelike  $\theta$  profile than the MPC control. This is due to the utilizations of different  $\theta_{\text{max}}$  at 2000 rpm/3 bar ( $\theta_{\text{max}} = 0.15$  for MPC and  $\theta_{max} = 0.25$  for the baseline control). Since the simulated UDDS cycle was dominated by the low-BMEP operation, the NH<sub>3</sub> produced at 2000 rpm/8 bar is insufficient for reducing all NO<sub>x</sub> emissions at 2000 rpm/3 bar. Therefore, NH<sub>3</sub> generation at 2000 rpm/3 bar is also required for NO<sub>x</sub> emission control. Utilizations of a smaller  $\theta_{\rm max}$  at 2000 rpm/3 bar and the terminal cost in the MPC control can avoid over production of NH<sub>3</sub>. In addition, the MPC control is capable of fully utilizing 2000 rpm/8 bar as the cost-effective NH<sub>3</sub> generation region. Consequentially, the MPC control can lower the fuel penalty associated with NH<sub>3</sub> generation by 32.0%, compared to the baseline control during this cycle. Furthermore, as summarized in Table 2, both controls can achieve over 96% NO<sub>x</sub> conversion efficiency and less than 15 ppm NH<sub>3</sub> slip on average during the simulated UDDS cycle.

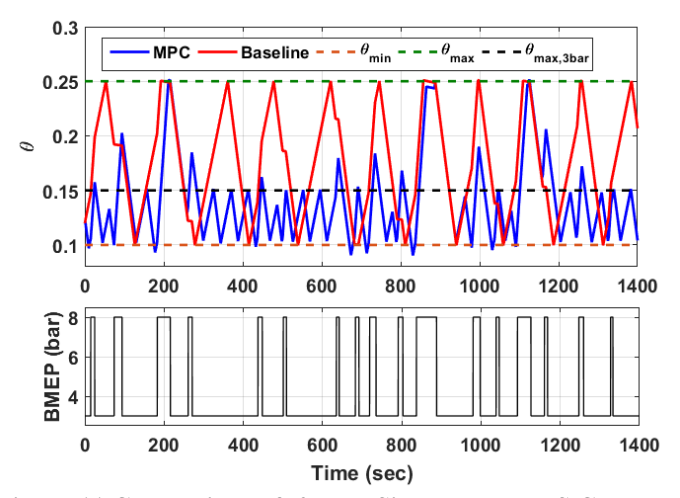


Figure 11 Comparison of  $\theta$  over Simulated UDDS Cycle.

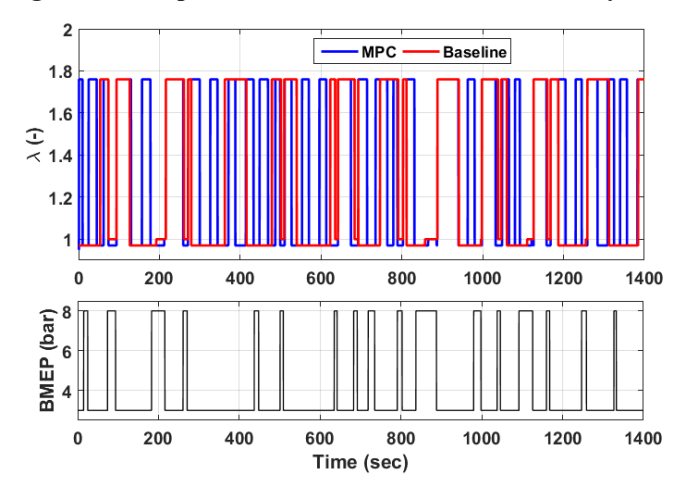


Figure 12 Comparison of  $\lambda$  over Simulated UDDS Cycle.

#### **CONCLUSIONS**

In this paper, engine experiments were conducted on a lean-burn gasoline coupled with a passive SCR system to identify the optimal  $\lambda$  for cost-effective NH<sub>3</sub> generation and highly efficient engine operation during NH<sub>3</sub> consumption mode. Then, an MPC-based mode switching control was systematically developed using the integrated engineaftertreatment system model for the lean-burn gasoline engine to minimize the fuel penalty associated with NH<sub>3</sub> generation and maximize the engine efficiency gain while satisfying stringent NO<sub>x</sub> and NH<sub>3</sub> emission requirements. Simulation results demonstrate that the MPC-based mode switching control is capable of reducing the corrected fuel penalty associated with NH<sub>3</sub> generation by 47.7% and 32.0% over the simulated US06 and UDDS cycles, respectively, compared to the baseline control, while achieving over 96% NO<sub>x</sub> reduction efficiency and less than 15 ppm average NH<sub>3</sub> slip. The benefits of the MPC-based control is more pronounced during US06 cycle than during UDDS cycle due to longer high-speed/high-load operation in US06 cycle. The simulation verification results indicate the potentials and benefits of the proposed MPC-based

mode-switching control in achieving high engine efficiency and stringent emissions requirements for lean gasoline engines with passive SCR system in transient driving cycles.

#### **REFERENCES**

- [1] U.S. Energy Information Administration, *Monthly Energy Review*. (DOE/EIA-0035), April 2016.
- [2] U.S. Environmental Protection Agency, *Inventory of U.S. Greenhouse Gas Emissions and Sinks: 1990–2014.* (EPA 430-R-16-002), April 2016.
- [3] T.V. Johnson, "Review of vehicular emissions trends," *SAE International Journal of Engines*, vol. 8, no. 3, pp. 1152-1167, 2015.
- [4] C.D. DiGiulio, J.A. Pihl, J.E.P. II, M.D. Amiridis and T.J. Toops, "Passive-ammonia selective catalytic reduction (SCR): Understanding NH<sub>3</sub> formation over close-coupled three way catalysts (TWC)," *Catalysis Today*, vol. 231, pp. 33-45, 2014.
- [5] W. Li, K.L. Perry, K. Narayanaswamy, C.H. Kim and P. Najt, "Passive ammonia SCR system for lean-burn SIDI engines," *SAE International Journal of Fuels and Lubricants*, vol. 3, no. 1, pp. 99-106, 2010.
- [6] J.R. Theis, J. Kim and G. Cavataio, "Passive TWC+SCR systems for satisfying tier 2, bin 2 emission standards on lean-burn gasoline engines," *SAE International Journal of Fuels and Lubricants*, vol. 8, no. 2, pp. 460-473, 2015.
- [7] V.Y. Prikhodko, J.E. Parks, J.A. Pihl and T.J. Toops, "Ammonia generation and utilization in a passive SCR (TWC+SCR) system on lean gasoline engine," *SAE International Journal of Engines*, vol. 9, no. 2016-01-0934, pp. 1289-1295 2016.
- [8] V.Y. Prikhodko, J.E. Parks, J.A. Pihl and T.J. Toops, "Passive SCR for lean gasoline NO<sub>x</sub> control: Engine-based strategies to minimize fuel penalty associated with catalytic NH<sub>3</sub> generation," *Catalysis Today*, vol. 267, pp. 202-209, 2016.
- [9] P. Chambon, S. Huff, K. Norman, K.D. Edwards, J. Thomas, and V. Prikhodko, "European lean gasoline direct injection vehicle benchmark," SAE Technical Paper 2011-01-1218, 2011.
- [10] M. Hsieh and J. Wang, "Development and experimental studies of a control-oriented SCR model for a two-catalyst urea-SCR system," *Control Eng.Pract.*, vol. 19, no. 4, pp. 409-422, 2011.
- [11] P. Chen and J. Wang, "Estimation and adaptive nonlinear model predictive control of selective catalytic reduction systems in automotive applications," *J. Process Control*, vol. 40, pp. 78-92 2016.